NAIRscore as a biomarker for the quality of immune response to neoantigens is related with an increased overall survival in multiple myeloma

Xingxing Jian,[1,6] Linfeng Xu,[2,4] Jingjing Zhao,[2,5] Yanhui Wang,[5] Wen Zhou,[3] and Lu Xie[1,2,6]

[1]Bioinformatics Center & National Clinical Research Centre for Geriatric Disorders & Department of Geriatrics, Xiangya Hospital, Central South University, Changsha, Hunan, China; [2]Shanghai-MOST Key Laboratory of Health and Disease Genomics, Institute for Genome and Bioinformatics, Shanghai Institute for Biomedical and Pharmaceutical Technologies, Shanghai, China; [3]Key Laboratory of Carcinogenesis of the Chinese Ministry of Health, The Key Laboratory of Carcinogenesis and Cancer Invasion of the Chinese Ministry of Education, Cancer Research Institute, School of Basic Medical Sciences, Central South University, Changsha, Hunan, China; [4]School of Medical Instrument and Food Engineering, University of Shanghai for Science and Technology, Shanghai, China; [5]College of Food Science and Technology, Shanghai Ocean University, Shanghai, China

Neoantigen provides a promising breakthrough in tumor immunotherapy, although only a subset of patients responds well due to the quality of their immune response. However, few biomarkers have been reported to measure the quality of immune response to neoantigens and to predict prognosis of patients with multiple myeloma (MM). Here, we first developed a neoantigen-prediction pipeline starting from outcomes of somatic mutations and gene-expression profiles. Given the expression of some specific marker genes, the human leukocyte antigen (HLA)-I score and the cytolytic score were evaluated respectively to reflect HLA-I molecular expression and CD8+ T/natural killer (NK) cell abundance. According to the process of the immune response to neoantigens, we comprehensively took neoantigen load, cytolytic score, and HLA-I score to construct a neoantigen immune response score (*NAIRscore*), in which the HLA-I score presented a hazard ratio (HR) of less than 1, while the cytolytic score and neoantigen load presented a HR of greater than 1. Meanwhile, *NAIRscore* presented a competitive advantage to stratify MM samples. Especially, those exhibiting high *NAIRscore* correlated with an increased overall survival (OS), echoing the underlying molecular signatures of lower driver-gene mutations and down-regulated immune response. Notably, an online tool based on this study is provided to identify neoantigens and predict OS.

INTRODUCTION

Multiple myeloma (MM) is the second most frequent hematological malignancy as characterized by the clonal expansion of malignant plasma cells within bone marrow, affecting >30,000 individuals per year in the United States.[1,2] In recent decades, many explorations and advances in therapeutics have prolonged the survival for most patients with MM, but MM remains incurable and prone to relapse in the vast majority of cases.[3-6] The treatment of MM remains challenging, especially for relapsed/refractory patients. Due to clinical and pathological heterogeneity, response and survival in MM treatment vary to prognostic risk factors, such as disease stage at diagnosis and cytogenetic abnormalities.[7,8] Therefore, correlating prognostic factors with biological function could enable the development of novel and targeted therapeutic classes.

In recent years, cancer immunotherapy with neoantigen vaccines has been considered a promising strategy for stimulating the body's own immune system to eliminate tumor cells; however, only small subsets of patients within large cohorts favorably respond to the treatment due to the quality of their immune response.[9,10] Neoantigens are a class of short peptides with aberrant expression in tumor cells, which result from somatic mutations and are used as tumor-specific antigens. Therein, neoantigens can bind to human leukocyte antigen (HLA) molecules and be presented on the surface, thereby being recognized as non-self by T cell receptors (TCRs) to elicit a T cell-mediated anti-tumor immune response.[11,12] Previously, our team developed a customized proteogenomic workflow for neoantigen prediction and selection, i.e., ProGeo-neo,[13] and we recently updated this tool (v.2.0) for expanding the source of candidate neoantigens.[14] Also, we issued a manually curated database of human tumor neoantigen peptides, i.e., dbPepNeo,[15] which helps screen immunogenic neoantigens from candidates. This database was updated recently to v.2.0.[16] Besides, we have developed additional tools for identification of immunogenic neoantigens and for the subsequent design of candidate peptide vaccines.[17-19]

Table 1. Clinical characteristics of 516 samples used in this study

	Primary (n = 462)	Recurrent (n = 54)
Age (years)		
Mean	65.2	68.1
SD	10.5	10.4
Gender (%)		
Male	283 (61.3)	26 (48.1)
Female	179 (38.7)	28 (51.9)
Race (%)		
White	462 (100)	54 (100)
ISS stage (%)		
I	152 (32.9)	14 (25.9)
II	154 (33.3)	17 (31.5)
III	140 (30.3)	22 (40.7)
NA	16 (3.5)	1 (1.9)

SD, standard deviation; ISS, International Staging System; NA, not available.

Several clinical trials have shown that personalized neoantigen vaccines have the ability to induce CD8+ and CD4+ T cell responses and improve the overall survival of patients with melanoma and glioblastoma, highlighting the considerable potential of neoantigen used in immunotherapy.[20,21] In addition, neoantigen load was correlated with somatic mutations, and both were reported to relate to prolonged survival with checkpoint inhibitors in melanoma and lung cancer.[22,23] High tumor mutational burden (H-TMB) has received FDA approval for selecting suitable patients for immunotherapy;[24] however, little has been reported with regard to low-TMB cancers, such as MM. Studies have shown that the quality of immune response to neoantigens may act as a better biomarker for immunotherapy.[10,25]

Here, based on the 516 paired outcomes (i.e., Maf and FPKM files) of 478 patients with MM downloaded from the MMRF-CoMMpass project, we developed a neoantigen-prediction pipeline to identify neoantigens in each tumor. Then, to represent the quality of immune response to neoantigens, we took the neoantigen load, the cytolytic score, and the HLA-I score to construct a neoantigen immune response score (*NAIRscore*). A high *NAIRscore* was found to be associated with an increased overall survival. For ease of use by clinicians, based on this study, we have established a friendly web-based tool with URL at http://www.biostatistics.online/MMPrgognosis/.

RESULT
Higher mutation burden and neoantigen load in recurrent patients compared with primary patients
In this study, based on the MMRF-CommPass project on the GDC data portal, we downloaded 1,092 simple nucleotide variation files (i.e., Maf) and 859 transcriptomic profiles (i.e., FPKM), respectively. These files were derived from whole-exon sequencing (WES) and RNA sequencing (RNA-seq) of CD138+ cells from patients with myeloma, respectively. As shown in Figure S1, after sample selection,

a total of 516 matched Maf files and FPKM files derived from 478 patients with MM were retained, including 462 primary samples and 54 recurrent samples (Table 1). In particular, paired primary and recurrent samples from 32 patients with MM were simultaneously obtained.

We first carried out analysis of somatic mutations in 516 Maf files using R package maftools.[26] In 462 primary samples, a total of 27,953 nonsynonymous variations were detected, ranging from 5 to 1,864 variations per sample, with a median of 46 variations (Figure S2A). Similarly, in 54 recurrent samples, a total of 3,815 nonsynonymous variations were identified, ranging from 4 to 207 variations per sample, with a median of 60 variations (Figure S2B). Comparatively, more nonsynonymous mutations were found in recurrent samples (Figure 1A). And, in recurrent samples, significantly higher TMB was observed as well (Figure 1B). When compared with the 33 TCGA tumors cohorts by function "tcgaCompare" of R package maftools,[26] MM expresses as a low-TMB tumor (Figure S3).

As shown in Figure S1, a workflow for predicting neoantigens starting with the Maf file and the FPKM file was established through referring to the published neoantigen-prediction pipeline.[27] As the nonsynonymous variations in chromosomes may lead to the changes in amino acid sequences of mutated genes in various forms, including single amino acid variation (SAAV), insertion or deletion of amino acids (indelAA), and frameshift mutation of amino acids (FSAA). Based on the mutated genes and their altered amino acids, the 8–11 amino acid short peptides containing those changed amino acid(s) were computationally cut from the reference amino acid sequence of mutated genes, and then their binding to HLA type was separately predicted for each patient. HLA-A·02:01 was applied to all patients with MM, as this HLA type is most prevalent among White people in the United States, according to the Allele Frequency Net Database (AFND).[28]

Statistically, a total of 6,329 neoantigens were identified in 462 primary samples, ranging between 1 and 437 per sample, with a median of 10. In 54 recurrent samples, a total of 887 neoantigens were identified, ranging between 1 and 65 per sample, with a median of 12. Here, we directly defined the number of neoantigens as neoantigen load in each sample. Comparatively, a significantly higher neoantigen load in recurrent samples was observed when compared with the primary samples (Figure 1C). Also, a higher neoantigen load was found when comparing those recurrent samples with their paired primary samples (Figure 1D). Furthermore, when we compared those samples diagnosed at different International Staging System (ISS) stages, no significance was observed on neoantigen load in primary and recurrent samples (Figures S4A and S4B), suggesting that the production of neoantigens has no significant correlation with ISS stage.

In addition, in both primary (Figure 1E) and recurrent (Figure 1F) samples, a significant positive correlation was discovered between the nonsynonymous mutations and neoantigen load. Additional nonsynonymous mutations may be responsible for relapse in recurrent patients. At the same time, in recurrent samples, more
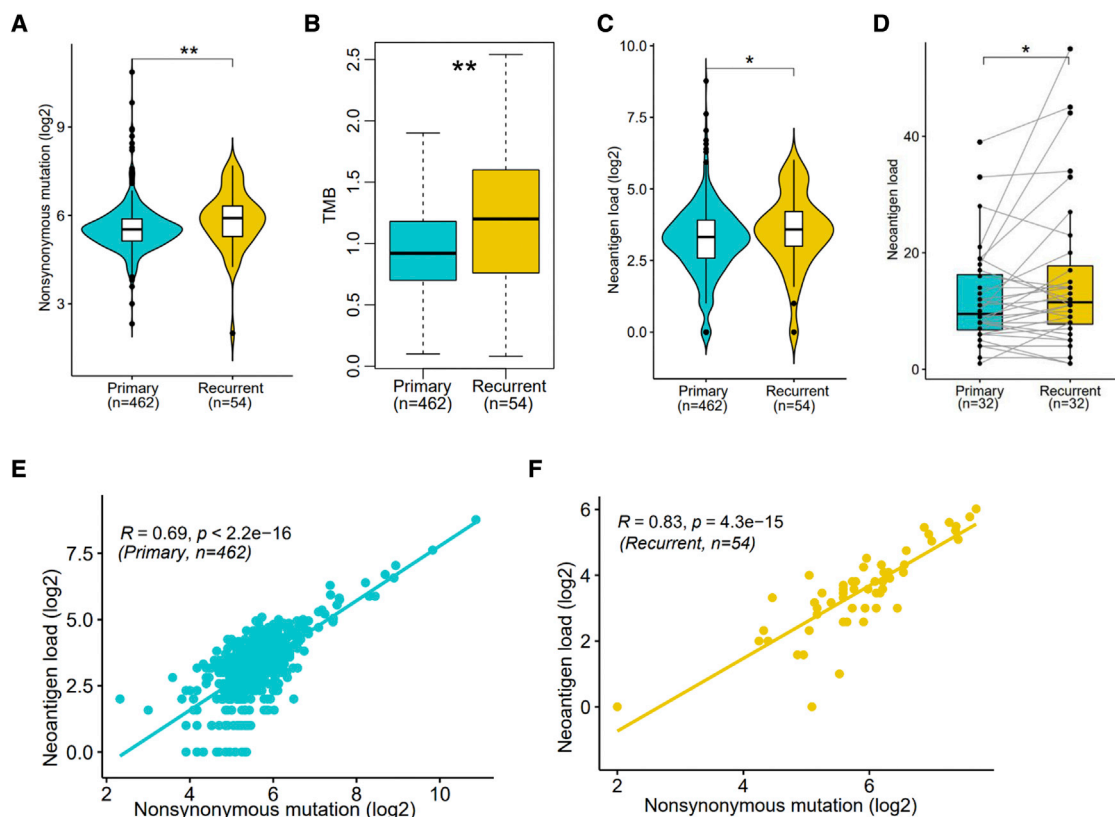
Figure 1. Comparison of characteristics between recurrent and primary samples

(A–C) Comparison of nonsynonymous mutation (A), TMB (B), and neoantigen load (C) between primary and recurrent samples. (D) Comparison of neoantigen load between primary and paired recurrent samples. (E and F) The Pearson's correlation between nonsynonymous mutations and neoantigen load in primary (E) and recurrent (F) samples. Significance was determined by Wilcoxon test. *p < 0.05, **p < 0.01.

nonsynonymous mutations resulted in a relatively higher TMB, but this may also lead to production of more neoantigens. Consistent with the top mutated genes (Figures S2A and S2B), we found that the neoantigens' peptides were predominantly derived from immunoglobulin heavy- and light-chain genes *IRF4* and *TP53*.

A high *NAIRscore* was related to an increased overall survival

Neoantigens are considered a class of tumor-specific antigens that can bind to HLA moleculars and present on the surface of tumor cells, thereby being recognized specifically by T cells.[12] Since only HLA-I neoantigens were predicted in this study, we took HLA-I molecular expression and CD8+ T cell abundance into consideration. In light of the expression level of some specific marker genes according to a prior study,[29] the HLA-I score and the cytolytic score can be evaluated to represent HLA-I molecular expression and CD8+ T cell abundance in each sample, respectively. Marker genes *B2M*, *HLA-A*, *HLA-B*, and *HLA-C* were used to evaluate the HLA-I score, while marker genes *GZMA*, *GZMH*, *PRF1*, *GNLY*, and *GZMM* were used to calculate the cytolytic score.

Given the process of immune response to neoantigens, we used the cytolytic score, the HLA-I score, and neoantigen load to construct a *NAIRscore* to measure the quality of immune response to tumor neoantigens by performing a multivariable Cox proportional hazards regression model. As shown in Figure 2A, we observed that the median of *NAIRscore* significantly stratified samples into high- and low-*NAIRscore* groups, and the high-*NAIRscore* group was associated with an increased overall survival (OS) (hazard ratio [HR] = 0.37; log rank test, p = 0.0014). Due to the significant difference in neoantigen load between primary and recurrent samples above, the *NAIRscore* was separately applied for sample stratification. With one accord, high *NAIRscore*s were observed to relate to an increased OS in both recurrent (Figure 2B; *HR* = 0.07, p = 3e-04) and primary samples (Figure 2C; *HR* = 0.52, p = 0.0667), although there was no significance in primary samples.

To further investigate the association between *NAIRscore* and OS in primary samples, we divided those primary samples into four quartiles based on the rank of the *NAIRscore* (Figure 2D). Interestingly, those primary samples in the third and fourth quartiles can both be divided significantly into high- and low-*NAIRscore* groups by the median *NAIRscore*, respectively (Figures 2E and 2F), and the high-*NAIRscore* group exhibited better OS. In contrast, those primary samples in the first and second quartiles cannot both be significantly stratified by
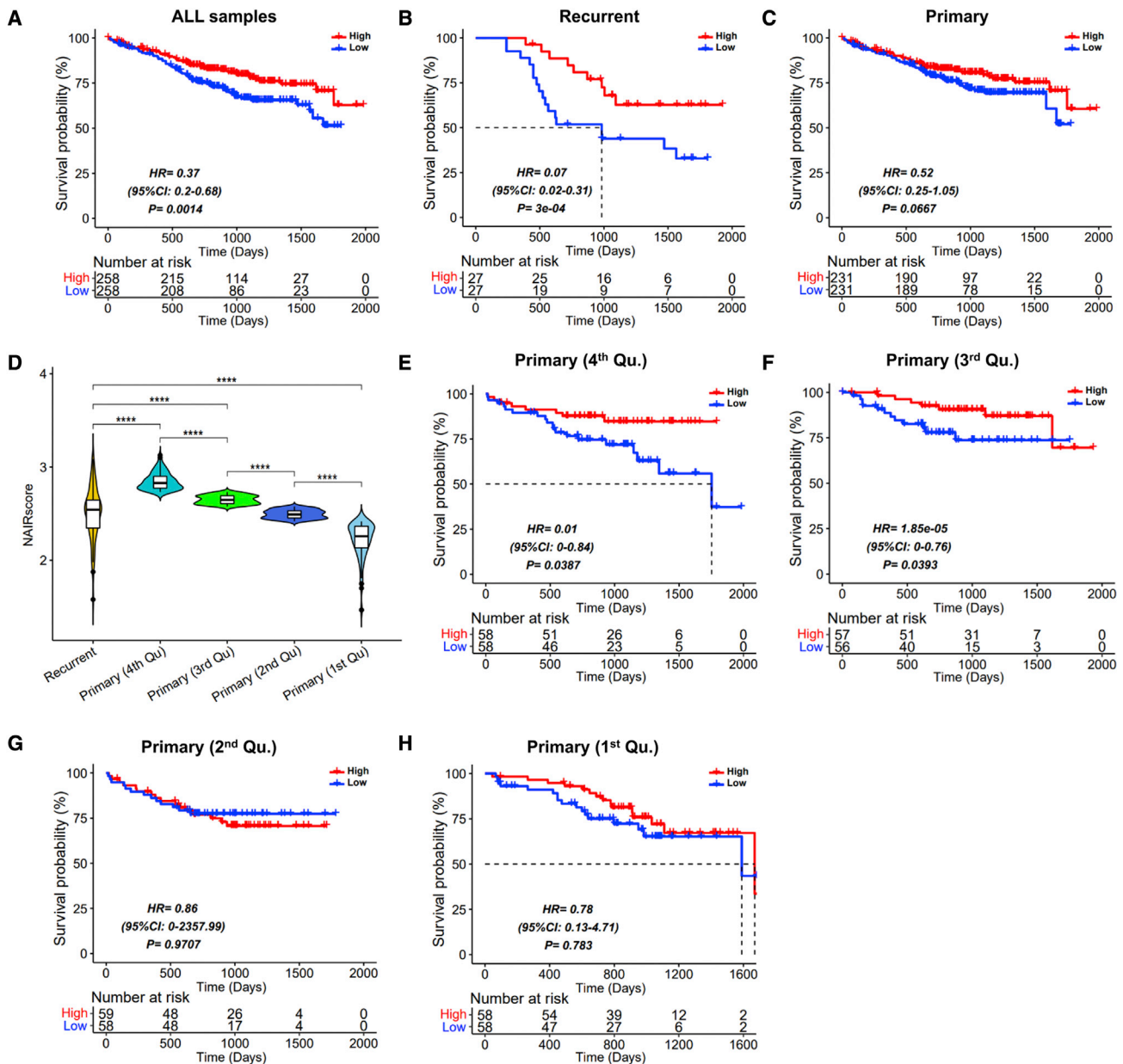
**Figure 2. Prognostic analysis in different subsets of patients with MM**

The median of *NAIRscore* in each prognostic model was used to divide samples into high- and low-*NAIRscore* groups. (A–C) Prognostic analysis in all samples (A), recurrent samples (B), and primary samples (C). (D) Comparison of *NAIRscore* between the recurrent samples and the four quartiles of primary samples. (E–H) Prognostic analysis in the fourth quartile (Qu.) (E), third Qu. (F), second Qu. (G), and first Qu. (H) in primary samples.

the median of their *NAIRscore* (Figures 2G and 2H). However, when those primary samples in the first and second quartiles were further differentiated between high- and low-*NAIRscore* groups by the optimal p value, respectively, we also observed that the high-*NAIRscore* group exhibited better outcomes (Figures S5A and S4B). Indeed, the quality of immune response to tumor antigens can play a pivotal role in survival.[10] In addition, we also considered that the *NAIRscore*

has no significant correlation with the ISS stage, as the comparisons presented in Figures S4C and S4D reveal.

NAIRscore as a biomarker has a competitive advantage

Considering the observation of significant stratification in recurrent samples and in the third and fourth quartiles of those primary samples above, we merged these samples to re-construct *NAIRscore* by
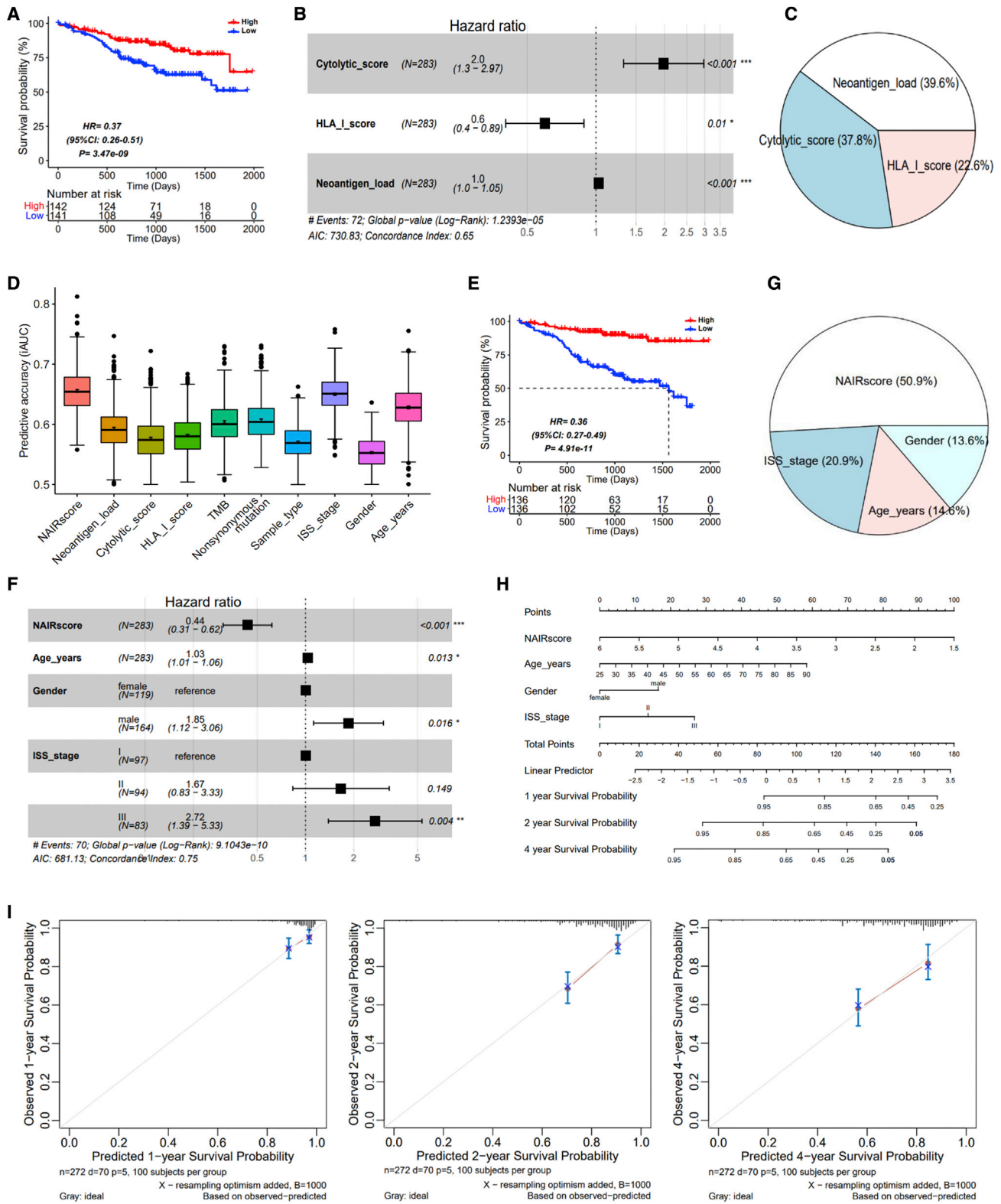
re-computing a multivariable Cox regression model. Expectedly, these samples were significantly stratified into high- and low-*NAIRscore* groups, and the high-*NAIRscore* group was found to be associated with increased OS (Figure 3A). Consequently, in the subgroups of MM samples, i.e., ISS stage, gender, and age, *NAIRscore* can be used as an effective biomarker for sample stratification, and a high *NAIRscore* was associated with an increased OS (Figures S6A–S6C). In addition, in this fitted Cox model, a competitive concordance index was measured, and the three features were all significant (Figure 3B). Therein, an HLA-I score with an HR of less than 1 indicated that the higher expression of the HLA-I molecular expression, the more conducive to the patients' OS. In contrast, a cytolytic score and neoantigen load with an HR of greater than 1 indicated that the higher value of cytolytic score and neoantigen load, the worse the patients' OS. Meanwhile, the relative contribution of each variable in this model was estimated (Figure 3C), suggesting that the three variables all critically contribute to construct *NAIRscore*.

Furthermore, by performing a 1,000× bootstrap resampling to calculate the integrated area under the receiver operating characteristic (ROC) curve (iAUC), we further compared the predictive accuracy of *NAIRscore* with other factors. As shown in Figure 3D, the iAUCs of *NAIRscore* and ISS stage were comparable, and both were superior to the other features. Interestingly, neoantigen load, TMB, and non-synonymous mutation were found to yield the same iAUC, suggesting that they had similar predictive accuracy, possibly due to their correlation.

Moreover, combining *NAIRscore* with three clinical features, i.e., ISS type, gender, and age, we further carried out a prognostic analysis and fitted the *SCORE*. Uniformly, when the median of *SCORE* were used to divide those samples into high- and low-*SCORE* groups, much smaller p values were observed (Figure 3E). In the forest plot shown in Figure 3F, we observed a larger concordance index, indicating that the addition of clinical features improved the predictive power. Meanwhile, as shown in Figure 3G, *NAIRscore* was found to make a greater contribution to this model, followed by ISS stage, age, and gender. In addition, a nomogram was constructed for clinicians, illustrating that a quantitative probability can be evaluated in predicting 1-, 2-, and 4-year OS for an individual (Figure 3H). The calibration curves of the nomogram in predicting 1-, 2-, and 4-year survival rates were also validated (Figure 3I), suggesting that a good predictive robustness can be achieved using this nomogram. Also, the *NAIRscore* was observed to contribute the most risk points when compared with others, indicating that the *NAIRscore* was a more important feature.

Comparison of molecular characteristics between high- and low-*NAIRscore* groups

To explore the underlying molecular characteristics of different OSs between samples with high and low *NAIRscore*s, we separately compared their somatic mutations and differentially expressed genes (DEGs). Primarily, driver genes in high- and low-*NAIRscore* groups were identified (Figures 4A and 4B). Meanwhile, genes *NRAS*, *KRAS*, and *BRAF* were considered as drivers in both high- and low-*NAIRscore* groups. In the low-*NAIRscore* group, however, we identified more driver genes, especially genes *KRAS*, *TP53*, and *IRF4* with higher mutational frequency (Figure 4C), which may explain in part the poor prognosis in the low-*NAIRscore* group. Compared with wild-type samples, samples with *KRAS* mutant (Figure 4D) and samples with *TP53* mutant (Figure 4E) all exhibited a decreased survival. Indeed, *KRAS* mutation was reported to relate to tumor-promoting inflammation and immune modulation, leading to immune escape in the tumor microenvironment.[30,31] The loss or mutation of *TP53* resulted in immune evasion by affecting the activity of myeloid and T cells and modulating the immune response during cancer development.[32] The transcription factor *IRF4* is required during immune response, including lymphocyte activation and the generation of immunoglobulin-secreting plasma cells.[33]

Moreover, the DEGs between high and low*NAIRscore*s were investigated as well. As shown in Figure 4F, we identified 14 up-regulated genes and 171 down-regulated genes in total (Table S1). In particular, genes *GZMA*, *GZMH*, *GNLY*, and *PRF1* marked to the cytolytic score were down-regulated in the high-*NAIRscore* group. Therefore, lower cytolytic scores were evaluated in the high-*NAIRscore* group, which corresponded to the cytolytic score with an HR greater than 1 (Figure 3B). Further, these down-regulated DEGs in the high-*NAIRscore* group were applied for GO enrichment analysis (Table S2). Consistently, several significant biology processes (BPs) with regard to immune response were enriched (Figure 4G), such as T cell activation, immune-response-activating cell-surface receptor signaling pathway, antigen-receptor-mediated signaling pathway, and regulation of T cell activation. The cell component (CC) and molecular function (MF) also were enriched, including TCR complex, antigen binding, TCR binding, and major histocompatibility complex (MHC) class I protein binding. More specifically, these down-regulated immune response induced by neoantigens may lead to better survival in the high-*NAIRscore* group.

A web-based tool to identify neoantigens and predict OS for patients with MM

Based on the neoantigen-predictive pipeline proposed above and the prognostic model constructed by 516 patients with MM, we

---

Figure 3. Comparison of *NAIRscore* and other characteristics in a subset of samples, including the recurrent samples and the fourth Qu. and third Qu. primary samples

(A) Prognostic analysis based on *NAIRscore*. (B) The forest plot based on cytolytic score, HLA-I score, and neoantigen load. *p < 0.05, **p < 0.01, ***p < 0.001. (C) The relative contribution of cytolytic score, HLA-I score, and neoantigen load in prognostic model. (D) Comparison of predictive accuracy on between *NAIRscore* and other features. (E) Prognostic analysis based on *NAIRscore*, age, gender, and ISS stage. (F) The forest plot based on *NAIRscore*, age, gender, and ISS stage. *p < 0.05, **p < 0.01, ***p < 0.001. (G) The relative contribution of *NAIRscore*, age, gender, and ISS stage in prognostic model. (H) Nomogram for predicting the 1-, 2-, and 4-year OS probabilities. (I) Calibration curves for 1-, 2-, and 4-year OS.
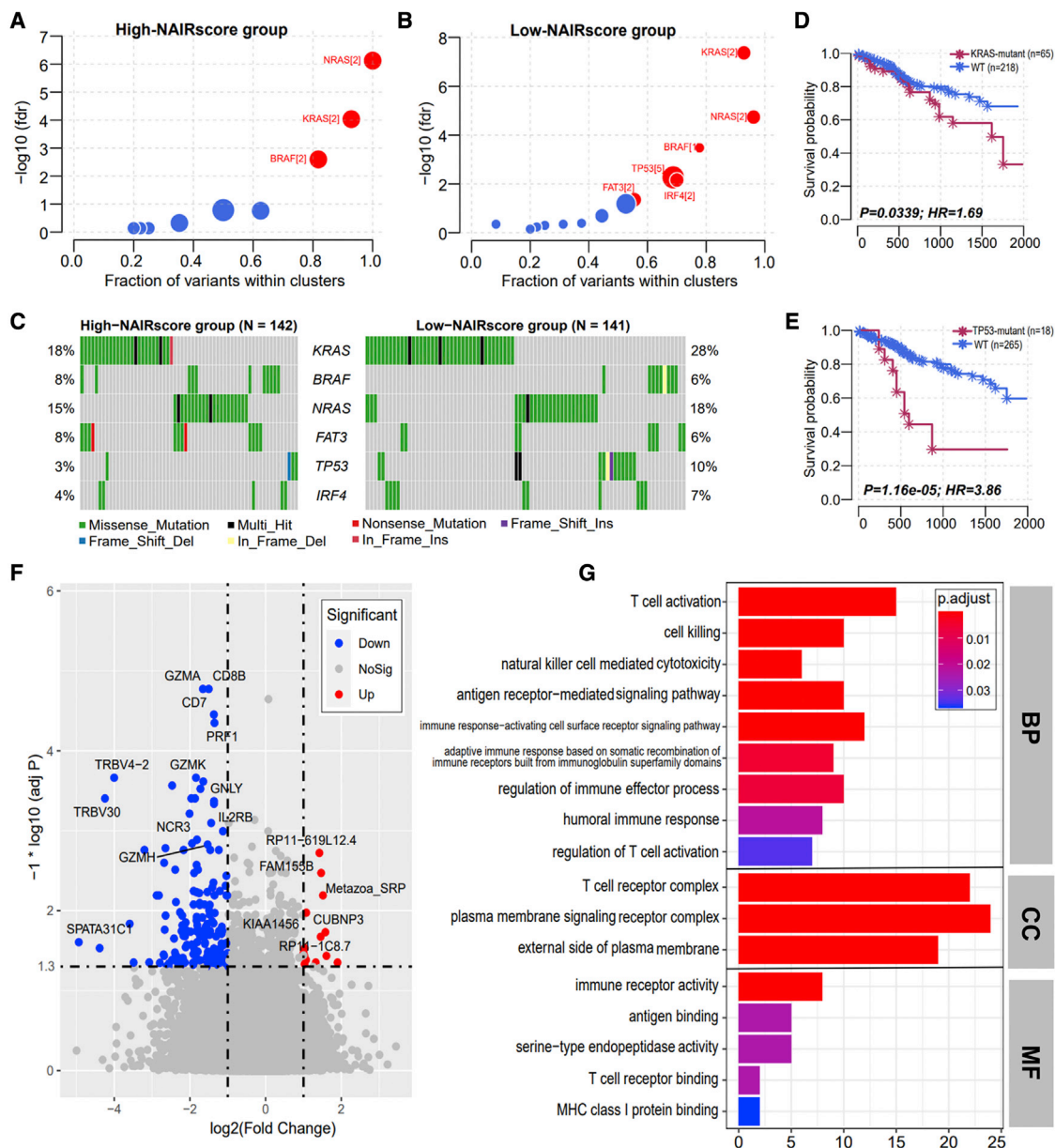
Figure 4. Molecular characteristics between high- and low-*NAIRscore* groups

(A and B) The driver genes identified in samples of high- (A) and low-*NAIRscore* group (B). (C) The mutational waterfall of driver genes in samples of high- and low-*NAIRscore* groups. (D) Prognostic analysis in samples with *KRAS* mutant. (E) Prognostic analysis in samples with *TP53* mutant. (F) The up- and down-regulated genes between high- and low-*NAIRscore* groups. (G) The GO enrichment analysis of the down-regulated genes, including biological process (BP), cellular component (CC), and molecular function (MF).

developed a web-based tool to identify neoantigens and predict the OS for each patient with MM (http://www.biostatistics.online/MMPrgognosis/). In this tool, users need to provide two text files from the same patient with MM patient, i.e., a Maf file to reflect somatic mutations in tumor and an FPKM file to represent expression level of genes in tumor. After uploading the two files, those neoantigens in the tumor can be identified within several minutes, and users

can directly download results for further exploration, such as personalized neoantigen vaccines. In the meantime, users also can obtain the predictive OS table and risk curve.

In this tool, the scoring system of *NAIRscore* was fitted as follow: $(-1 \times 0.3222 \times \text{cytolytic score}) + [-1 \times (-0.2699) \times \text{HLA-I score}] + (-1 \times 0.0021 \times \text{neoantigen load})$, and the median *NAIRscore* in this

study (2.5686) was used to divide patients into high- and low-*NAIR-score* groups. The patients with a *NAIRscore* greater than 2.5686 would exhibit a high OS rate. The OS rate at different time points could be calculated and presented in the table and curve. Moreover, if three clinical features, i.e., ISS stage, age, and gender, were provided by users, the scoring system would be further upgraded as follow: $(-1 \times 0.7009 \times NAIRscore) + (-1 \times 0.0316 \times age) + [-1 \times (0_{female} \mid 0.3634_{male})] + [-1 \times (0_{ISS-I} \mid 0.9343_{ISS-II} \mid 1.4124_{ISS-III})]$. Similarly, the median *SCORE* (-1.3509) was used to stratify samples and predict OS. Importantly, this tool is easy to operate and is user friendly for clinicians, which is very helpful for the generalization and application of our models.

DISCUSSION

In this study, an effective neoantigen-prediction pipeline starting from Maf and FPKM profiles was proposed and integrated into a web-based tool, in which neoantigens resulted from somatic mutations can be identified within minutes. It can serve as an alternative when raw sequencing data is not available. Here, consistent with a prior report,[34] we found that larger mutational burden and neoantigens load in recurrent MM samples compared with the primary MM samples. This indicated that the larger mutational burden may be the cause of relapse in recurrent patients, as well as more neoantigen production.

According to the process of immune response to tumor antigens, we treated neoantigen load, the HLA-I score, and the cytolytic score as features to construct the *NAIRscore*, representing the quality of immune response to tumor antigens in samples. Meanwhile, we observed that neoantigen load and the cytolytic score have HRs of greater than 1, and the HLA-I score has an HR of less than 1. Consistently, neoantigen load has been reported as an HR of greater than 1, and high somatic mutation and neoantigen load were correlated with decreased progression-free survival in MM.[35] These suggested that a higher cytolytic score resulting from neoantigen load did not yield a better prognosis in MM, although a high neoantigen load and tumor-infiltrating CD8+ T cells have been reported to imply a better survival in some solid tumors, such as melanoma and neuroblastoma.[36,37] This might indicate a difference between low- and high-TMB tumors.

In addition, patients whose samples had a high *NAIRscore* were found to be significantly associated with a better OS, indicating that this is consistent with previous research that a high quality of immune response to tumor antigens was beneficial to prognosis.[10] In particular, we found that the *NAIRscore* was able to significantly stratify those MM samples with a high *NAIRscore*. That suggests that a comprehensive consideration of immune response processes may better serve as a biomarker, rather than any one individually, i.e., neoantigen load, tumor-infiltrating CD8+ T cells, and HLA molecular expression. Indeed, in the high-*NAIRscore* group, we observed fewer driver genes, such as *KRAS*, *TP53*, and *IRF4*, and a down-regulated BP of immune response induced by neoantigens, such as immune-response-activating cell-surface receptor signaling pathway and antigen-receptor-mediated signaling pathway. Of course, in the future,

NAIRscore needs to be validated in more MM samples, including taking monoclonal gammopathy of undetermined significance (MGUS) and smoldering MM (SMM) into account. Especially, *NAIRscore* needs to be verified and compared in more tumors, including high- and low-TMB tumors.

As we have known, H-TMB has received FDA approvals for selecting patients for promising immune checkpoint inhibitor (ICI) treatment. However, compared with TMB, neoantigen load was observed to be of equal advantage, while *NAIRscore* presented a greater advantage (Figure 3D). TMB refers to the number of somatic mutations per megabase of interrogated genomic sequence, while neoantigens denote those immunogenic short peptides originated from somatic mutations. To some extent, TMB and neoantigen load are all positively correlated with somatic mutations in tumor. Meanwhile, emerging research showed that the quality of the immune response is more important in tumors,[10] which may explain why *NAIRscore* exhibits a better advantage.

In summary, we constructed *NAIRscore* for the first time to evaluate the quality of immune response to tumor neoantigens, in which a high *NAIRscore* was found to be an effective biomarker to relate with increased OS. A friendly web-based tool was implemented to identify neoantigens and predict prognosis for patients with MM.

MATERIALS AND METHODS

Sample collection and selection

In this study, open sequencing files of CD138+ cells from patients with MM were downloaded from the MMRF-CoMMpass project (dbGaP study accession: phs000748) through the GDC data portal (https://portal.gdc.cancer.gov/projects/MMRF-COMMPASS), including WES and RNA-seq (Figure S1). We obtained 1,092 simple nucleotide variation files (Maf format) derived from WES and 859 transcriptomic profiles (FPKM) derived from RNA-seq. Here, we only retained the matched WES and RNA-seq samples with clinical information. Further, we selected those files sequenced from bone marrow samples from White patients with MM. Eventually, a total of 516 matched Maf files and FPKM files derived from 478 patients with MM were retained, including 462 primary samples and 54 recurrent samples. Therein, the paired primary and recurrent samples from 32 patients with MM were obtained simultaneously.

Sequencing and statistical analysis

As shown in GDC, the tumor cells (CD138+ cells sorted from bone marrow) and normal cells (whole blood cells from peripheral blood) from matched samples were evaluated by WES. Based on the workflow of aliquot ensemble somatic variant merging and masking and human reference genome (GRCh38), the simple nucleotide variations of each tumor sample were separately filtered and saved in Maf format. On the R (v.4.0.3) platform, the mutated classifications and mutated genes in each Maf file were filtered and analyzed by R package maftools (v.2.6.05),[26] the driver genes in different groups were implemented by the oncodrive function with mutations of greater than 8 and adjusted p values of less than 0.05.

In addition, the tumor cells were evaluated by RNA-seq, and the merged FPKM expression matrix was downloaded and used in this study. The FPKM matrix was applied for filtering of candidate neoantigens and evaluation of the cytolytic score and the HLA-I score.[29] The FPKM matrix was used to screen DEGs between groups by performing Wilcoxon rank-sum test and Benjamini-Hochberg (BH) adjustment, in which we set the cutoff at the absolute value of log2, a fold change of greater than 1, and an adjusted p value of less than 0.05.

Neoantigen-prediction pipeline

Referring to the published neoantigen-prediction pipeline,[27] as shown in Figure S1, we constructed a similar workflow for a neoantigen-prediction pipeline starting from Maf file and FPKM file. In this workflow, the mutated genes and their altered amino acids were first filtered from each Maf file. We downloaded the amino acid sequences of all human genes from UniprotKB. Then, based on those mutated genes and their altered amino acids, we can select those short peptides containing the mutated amino acids from their reference amino acid sequences. Only HLA-I neoantigens consisting of 8–11 amino acids were considered. Subsequently, the binding of these short peptides to HLA type was predicted by netMHCpan4.0,[38] and we screened those short peptides with %Rank of less than 2. Eventually, the expression level of genes mapped by those screening short peptides in the paired RNA-seq files was applied for selection, and we selected those peptides with FPKM of greater than 2.

Somatic mutations in chromosomes may lead to the changes in amino acid sequences of mutated genes in various forms, including SAAV, indelAA, or FSAA. For SAAV, we first found the mutant site in the amino acid sequence of the reference gene and replaced it with the mutant amino acid. Then, we can theoretically cut the sequence into 8–11 amino acid short peptides containing the mutated position. Similarly, for indelAA, we found the mutant site in the amino acid sequence of the reference gene and inserted or deleted the mutant amino acid(s). Also, those 8–11 amino acid short peptides containing the mutant amino acid(s) can be cut from the sequence. For FSAA, all mutant sites in the amino acid sequence of the reference gene were first identified, and the sequence containing these mutation sites was cut into 8–11 peptides.

Due to lack of sequence files (e.g., fastq), we cannot accurately predict HLA types for each patient with MM. In this study, as only White patients with MM were selected, according to the AFND,[28] we found that HLA-A·02:01 is the major HLA type among White people in the United States. Therefore, those short peptides were applied to predict the binding to HLA-A·02:01 by using netMHCpan4.0.

Evaluation of cytolytic score and HLA-I score

A previous report[29] showed that the cytolytic score and the HLA-I score in hematologic tumors can be evaluated by the geometric mean of expression of several specific marker genes as follows:

$$Cytolytic\ score\ =\ \sqrt[5]{\prod_{i=1}^{5} Marker_i}$$

$$HLA-I\ score\ =\ \sqrt[4]{\prod_{i=1}^{4} Marker_i},$$

in which i denotes the i-th marker genes. Accordingly, the marker genes GZMA, GZMH, PRF1, GNLY, and GZMM were used to calculate the cytolytic score, which is positively related to the cytolytic activity of CD8+ T/natural killer (NK) cells. The marker genes B2M, HLA-A, HLA-B, and HLA-C was used to detect the HLA-I score, which is significantly associated with the presentation of HLA-I neoantigens.

NAIRscore construction and prognostic analysis

In this study, we directly treated the number of neoantigens as neoantigen load in each sample. Taking neoantigen load, the cytolytic score, and the HLA-I score as features, a multivariable Cox proportional hazards regression model was constructed using the R package survival (v.3.2-13) and survminer (v.0.4.9), in which the coefficient (weight) of each feature can be generated in view of the importance of this feature. Meanwhile, NAIRscore can be constructed as follows:

$$NAIRscore\ =\ -1 \times \sum_{i=1}^{3} Coef_i \times Feature_i,$$

in which i denotes the i-th feature, and Feature and Coef represent its value and coefficient in the fitted model, respectively. The NAIRscore was designed to reflect the quality of immune response to neoantigens in each sample. We applied the median of NAIRscore to stratify samples into high- and low-NAIRscore groups.

Further, when combining NAIRscore and three clinical features, i.e., ISS stage, age, and gender, the scoring system was further upgraded as follows:

$$SCORE\ =\ -1 \times \sum_{i=1}^{4} Coef_i \times Feature_i,$$

in which i denotes the i-th feature. When the continuous features (i.e., NAIRscore, age) were applied, Feature and Coef represent its value and coefficient, respectively. When the feature was gender, "female" was treated as reference, and then "male" was applied by its Coef. When the feature was ISS stage, "ISS-I" was treated as reference, and then "ISS-II" and "ISS-III" were individually applied by their Coef.

The Kaplan-Meier survival curve was implemented by R package survminer (v.0.4.9), and the log rank test was used to compare the OS between high- and low-NAIRscore groups. The nomogram and calibration plots were visualized by using the R package rms (v.6.2-0).

To compare the predictive accuracy of the different variables or models, the iAUC with 100,00× bootstrap resampling was performed and analyzed. Referring to two previous studies,[39,40] the relative

contribution of each variable in the model was estimated by the proportion of overall χ2 from Harrell's rms R package (v.6.2-0). The R package compareC (v.1.3.2) was used to compare if the difference in two correlated overall concordance indices were statistically significant.

Establishment of online web tool

An easy-to-use web tool starting from the paired Maf and FPKM files was developed, which can allow users to identify neoantigens in tumor and predict a patient's OS. To implement an interaction interface and improve user experience, the front-end web framework was built by Bootstrap and Jquery, and the back-end was implemented by PHP.

DATA AVAILABILITY

All data used in this study were downloaded from project Multiple Myeloma CoMMpass Study (project ID: MMRF-COMMPASS; dbGaP study accession: phs000748) through the GDC data portal (https://portal.gdc.cancer.gov/projects/MMRF-COMMPASS).

SUPPLEMENTAL INFORMATION

Supplemental information can be found online at https://doi.org/10.1016/j.omtn.2022.07.006.

AUTHOR CONTRIBUTIONS

X.J. and L.X. conceived and designed this study. X.J. carried out data collection and analysis and wrote the draft manuscript. L.X. revised the manuscript. L.X. contributed to building the web-based tool. W.Z., J.Z., and Y.W. contributed to data analysis and interpretation. The authors read and approved the final manuscript.

DECLARATION OF INTEREST

The authors declare no competing interests.

REFERENCES

1. Kuehl, W.M., and Bergsagel, P.L. (2012). Molecular pathogenesis of multiple myeloma and its premalignant precursor. J. Clin. Invest. *122*, 3456–3463.

2. Siegel, R.L., Miller, K.D., Fuchs, H.E., and Jemal, A. (2021). Cancer statistics 2021. CA Cancer J. Clin. *71*, 7–33.

3. Roy, M., Liang, L., Xiao, X., Peng, Y., Luo, Y., Zhou, W., Zhang, J., Qiu, L., Zhang, S., Liu, F., et al. (2016). Lycorine downregulates HMGB1 to inhibit autophagy and enhances bortezomib activity in multiple myeloma. Theranostics *6*, 2209–2224.

4. Xia, J., He, Y., Meng, B., Chen, S., Zhang, J., Wu, X., Zhu, Y., Shen, Y., Feng, X., Guan, Y., et al. (2020). *NEK2* induces autophagy-mediated bortezomib resistance by stabilizing Beclin-1 in multiple myeloma. Mol. Oncol. *14*, 763–778.

5. Jian, X., Zhu, Y., Ouyang, J., Wang, Y., Lei, Q., Xia, J., Guan, Y., Zhang, J., Guo, J., He, Y., et al. (2020). Alterations of gut microbiome accelerate multiple myeloma progression by increasing the relative abundances of nitrogen-recycling bacteria. Microbiome *8*, 74.

6. Feng, X., Guo, J., An, G., Wu, Y., Liu, Z., Meng, B., He, N., Zhao, X., Chen, S., Zhu, Y., et al. (2022). Genetic aberrations and interaction of *NEK2* and *TP53* accelerate aggressiveness of multiple myeloma. Adv. Sci. *9*, e2104491.

7. Palumbo, A., Avet-Loiseau, H., Oliva, S., Lokhorst, H.M., Goldschmidt, H., Rosinol, L., Richardson, P., Caltagirone, S., Lahuerta, J.J., Facon, T., et al. (2015). Revised international staging system for multiple myeloma: a report from international myeloma working group. J. Clin. Oncol. *33*, 2863–2869.

8. Greipp, P.R., San Miguel, J., Durie, B.G.M., Crowley, J.J., Barlogie, B., Bladé, J., Boccadoro, M., Child, J.A., Avet-Loiseau, H., Harousseau, J.L., et al. (2005). International staging system for multiple myeloma. J. Clin. Oncol. *23*, 3412–3420.

9. Sambi, M., Bagheri, L., and Szewczuk, M.R. (2019). Current challenges in cancer immunotherapy: multimodal approaches to improve efficacy and patient response rates. J. Oncol. *2019*, e4508794.

10. Balachandran, V.P., Łuksza, M., Zhao, J.N., Makarov, V., Moral, J.A., Remark, R., Herbst, B., Askan, G., Bhanot, U., Senbabaoglu, Y., et al. (2017). Identification of unique neoantigen qualities in long-term survivors of pancreatic cancer. Nature *551*, 512–516.

11. Zhang, Z., Lu, M., Qin, Y., Gao, W., Tao, L., Su, W., and Zhong, J. (2021). Neoantigen: a new breakthrough in tumor immunotherapy. Front. Immunol. *12*, 672356.

12. Peng, M., Mo, Y., Wang, Y., Wu, P., Zhang, Y., Xiong, F., Guo, C., Wu, X., Li, Y., Li, X., et al. (2019). Neoantigen vaccine: an emerging tumor immunotherapy. Mol. Cancer *18*, 128.

13. Li, Y., Wang, G., Tan, X., Ouyang, J., Zhang, M., Song, X., Liu, Q., Leng, Q., Chen, L., and Xie, L. (2020). ProGeo-neo: a customized proteogenomic workflow for neoantigen prediction and selection. BMC Med. Genomics *13*, 52.

14. Liu, C., Zhang, Y., Jian, X., Tan, X., Lu, M., Ouyang, J., Liu, Z., Li, Y., Xu, L., Chen, L., et al. (2022). ProGeo-Neo v2.0: a one-stop software for neoantigen prediction and filtering based on the proteogenomics strategy. Genes *13*, 783.

15. Tan, X., Li, D., Huang, P., Jian, X., Wan, H., Wang, G., Li, Y., Ouyang, J., Lin, Y., and Xie, L. (2020). dbPepNeo: a manually curated database for human tumor neoantigen peptides. Database *2020*, baaa004.

16. Lu, M., Xu, L., Jian, X., Tan, X., Zhao, J., Liu, Z., Zhang, Y., Liu, C., Chen, L., Lin, Y., and Xie, L. (2022). dbPepNeo2.0: a database for human tumor neoantigen peptides from mass spectrometry and TCR recognition. Front. Immunol. *13*, 855976.

17. Wang, G., Li, Y., and Xie, L. (2019). Advances in the prediction of antigenic peptides in personalized tumor neoantigen vaccine. Prog. Biochem. Biophys. *46*, 441–448.

18. Zhao, J., Tan, X., Jian, X., Wang, G., and Xie, L. (2021). Bioinformatics prediction of candidate epitopes for peptide vaccines based on pathogen antigenic protein sequences. Life Sci. Res. *25*, 363–371.

19. Wang, G., Wan, H., Jian, X., Li, Y., Ouyang, J., Tan, X., Zhao, Y., Lin, Y., and Xie, L. (2020). INeo-Epp: a novel T-cell HLA class-I immunogenicity or neoantigenic epitope prediction method based on sequence-related amino acid features. BioMed Res. Int. *2020*, 5798356.

20. Ott, P.A., Hu, Z., Keskin, D.B., Shukla, S.A., Sun, J., Bozym, D.J., Zhang, W., Luoma, A., Giobbie-Hurder, A., Peter, L., et al. (2017). An immunogenic personal neoantigen vaccine for patients with melanoma. Nature *547*, 217–221.

21. Keskin, D.B., Anandappa, A.J., Sun, J., Tirosh, I., Mathewson, N.D., Li, S., Oliveira, G., Giobbie-Hurder, A., Felt, K., Gjini, E., et al. (2019). Neoantigen vaccine generates intratumoral T cell responses in phase Ib glioblastoma trial. Nature *565*, 234–239.

22. Van Allen, E.M., Miao, D., Schilling, B., Shukla, S.A., Blank, C., Zimmer, L., Sucker, A., Hillen, U., Foppen, M.H.G., Goldinger, S.M., et al. (2015). Genomic correlates of response to *CTLA-4* blockade in metastatic melanoma. Science *350*, 207–211.

23. Rizvi, N.A., Hellmann, M.D., Snyder, A., Kvistborg, P., Makarov, V., Havel, J.J., Lee, W., Yuan, J., Wong, P., Ho, T.S., et al. (2015). Mutational landscape determines sensitivity to PD-1 blockade in non-small cell lung cancer. Science *348*, 124–128.

24. Marcus, L., Fashoyin-Aje, L.A., Donoghue, M., Yuan, M., Rodriguez, L., Gallagher, P.S., Philip, R., Ghosh, S., Theoret, M.R., Beaver, J.A., et al. (2021). FDA approval

summary: pembrolizumab for the treatment of tumor mutational burden-high solid tumors. Clin. Cancer Res. *27*, 4685–4689.

25. Aurisicchio, L., Pallocca, M., Ciliberto, G., and Palombo, F. (2018). The perfect personalized cancer therapy: cancer vaccines against neoantigens. J. Exp. Clin. Cancer Res. *37*, 86.

26. Mayakonda, A., Lin, D.C., Assenov, Y., Plass, C., and Koeffler, H.P. (2018). Maftools: efficient and comprehensive analysis of somatic variants in cancer. Genome Res. *28*, 1747–1756.

27. Hundal, J., Carreno, B.M., Petti, A.A., Linette, G.P., Griffith, O.L., Mardis, E.R., and Griffith, M. (2016). pVAC-Seq: a genome-guided in silico approach to identifying tumor neoantigens. Genome Med. *8*, 11.

28. Gonzalez-Galarza, F.F., McCabe, A., Santos, E.J.M.D., Jones, J., Takeshita, L., Ortega-Rivera, N.D., Cid-Pavon, G.M.D., Ramsbottom, K., Ghattaoraya, G., Alfirevic, A., et al. (2020). Allele frequency net database (AFND) 2020 update: gold-standard data classification, open access genotype data and new query tools. Nucleic Acids Res. *48*, D783–D788.

29. Dufva, O., Pölönen, P., Brück, O., Keränen, M.A.I., Klievink, J., Mehtonen, J., Huuhtanen, J., Kumar, A., Malani, D., Siitonen, S., et al. (2020). Immunogenomic landscape of hematological malignancies. Cancer Cell *38*, 424–428.

30. Hamarsheh, S., Groß, O., Brummer, T., and Zeiser, R. (2020). Immune modulatory effects of oncogenic *KRAS* in cancer. Nat. Commun. *11*, 5439.

31. Ischenko, I., D'Amico, S., Rao, M., Li, J., Hayman, M.J., Powers, S., Petrenko, O., and Reich, N.C. (2021). *KRAS* drives immune evasion in a genetic model of pancreatic cancer. Nat. Commun. *12*, 1482.

32. Blagih, J., Buck, M.D., and Vousden, K.H. (2020). p53, cancer and the immune response. J. Cell. Sci. *133*, jcs237453.

33. Shaffer, A.L., Emre, N.C.T., Lamy, L., Ngo, V.N., Wright, G., Xiao, W., Powell, J., Dave, S., Yu, X., Zhao, H., et al. (2008). *IRF4* addiction in multiple myeloma. Nature *454*, 226–231.

34. Perumal, D., Imai, N., Laganà, A., Finnigan, J., Melnekoff, D., Leshchenko, V.V., Solovyov, A., Madduri, D., Chari, A., Cho, H.J., et al. (2020). Mutation-derived neoantigen-specific T-cell responses in multiple myeloma. Clin. Cancer Res. *26*, 450–464.

35. Miller, A., Asmann, Y., Cattaneo, L., Braggio, E., Keats, J., Auclair, D., Lonial, S., MMRF CoMMpass Network, Russell, S.J., and Stewart, A.K. (2017). High somatic mutation and neoantigen burden are correlated with decreased progression-free survival in multiple myeloma. Blood Cancer J. *7*, e612.

36. Spranger, S., Spaapen, R.M., Zha, Y., Williams, J., Meng, Y., Ha, T.T., and Gajewski, T.F. (2013). Up-regulation of PD-L1, Ido, and T(regs) in the melanoma tumor microenvironment is driven by CD8+ T cells. Sci. Transl. Med. *5*, 200ra116.

37. Bao, R., Spranger, S., Hernandez, K., Zha, Y., Pytel, P., Luke, J.J., Gajewski, T.F., Volchenboum, S.L., Cohn, S.L., and Desai, A.V. (2021). Immunogenomic determinants of tumor microenvironment correlate with superior survival in high-risk neuroblastoma. J. Immunother. Cancer *9*, e002417.

38. Jurtz, V., Paul, S., Andreatta, M., Marcatili, P., Peters, B., and Nielsen, M. (2017). NetMHCpan 4.0: improved peptide-MHC class I interaction predictions integrating eluted ligand and peptide binding affinity data. J. Immunother. *199*, 3360–3368.

39. Pagès, F., Mlecnik, B., Marliot, F., Bindea, G., Ou, F.-S., Bifulco, C., Lugli, A., Zlobec, I., Rau, T.T., Berger, M.D., et al. (2018). International validation of the consensus Immunoscore for the classification of colon cancer: a prognostic and accuracy study. Lancet *391*, 2128–2139.

40. Ren, J., Xu, L., Zhou, S., Ouyang, J., You, W., Sheng, N., Yan, L., Peng, D., Xie, L., and Wang, Z. (2021). Clinicopathological features combined with immune infiltration could well distinguish outcomes in stage II and stage III colorectal cancer: a retrospective study. Front. Oncol. *11*, 776997.